

Supporting Information

A novel quinolinyl-tetraphenylethene based fluorescence “turn-on” sensor for Zn²⁺ with a large Stokes shift and its applications for portable test strips and biological imaging

Jianxing Xu ^{1 a}, Jingwen Xiong ^{1 a}, Yanlin Qin*^a, Zongzhi Li ^a, Chengqiang Pan ^a,
Yanping Huo*^{ab}, Haoli Zhang ^{ac}

^a *School of Chemical Engineering and Light Industry, Guangdong University of
Technology, Guangzhou 510006, China*

^b *Guangdong Provincial Key Laboratory of Luminescence from Molecular Aggregates
(South China University of Technology), Guangzhou 510640, China*

^c *State Key Laboratory of Applied Organic Chemistry; Key Laboratory of Special
Function Materials and Structure Design; College of Chemistry and Chemical
Engineering, Lanzhou University, Lanzhou 730000, China*

* Corresponding author E-mail: yphuo@gdut.edu.cn (Y. Huo).

Table of contents

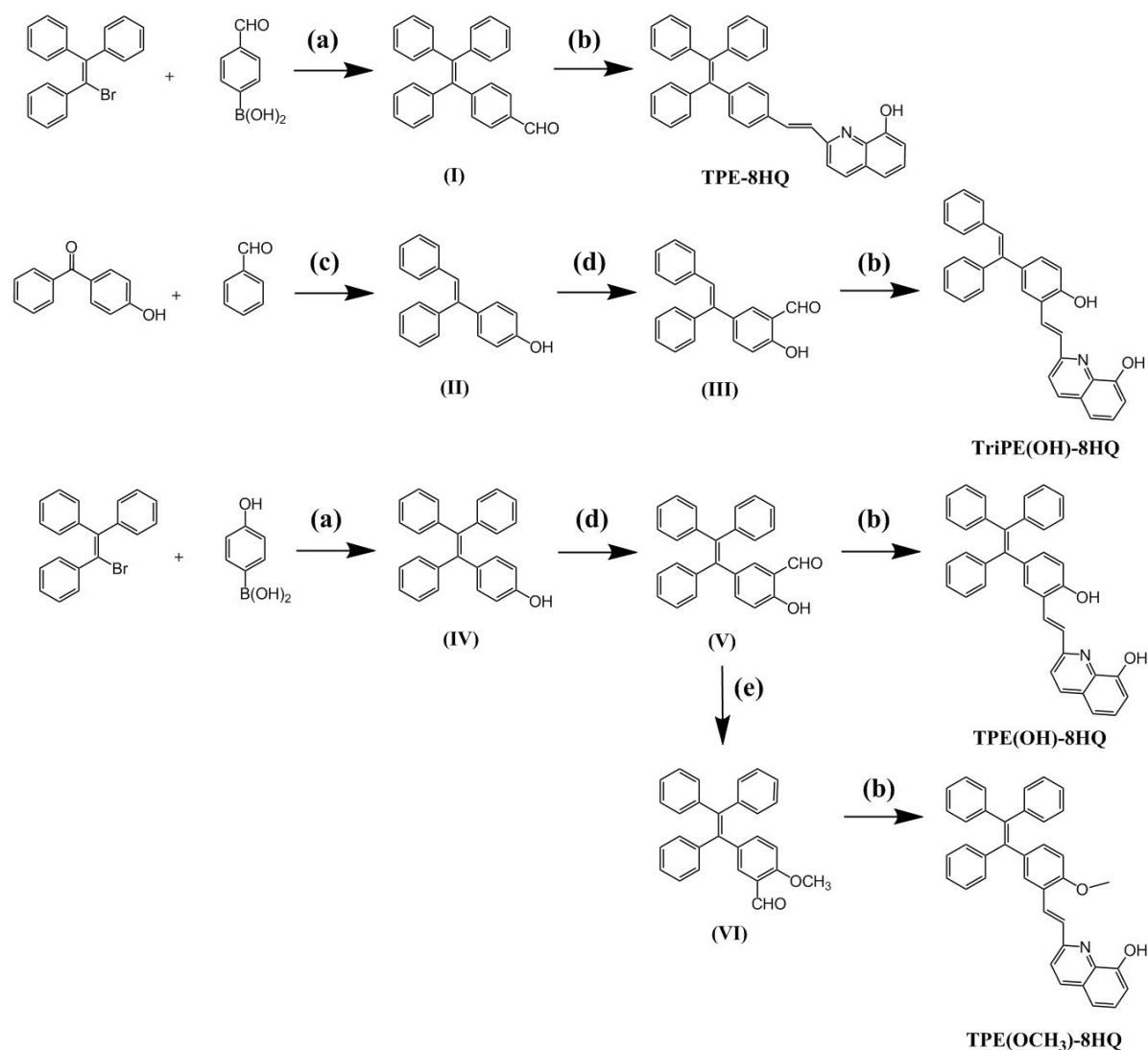
1. Experimental section
2. Synthesis routes and Characterization
3. IR spectrum of probe **TPE(OH)-8HQ**
4. DLS characterization of the **TPE-8HQ** in ethanol and mixed solvent
5. DLS characterization of the **TPE(OH)-8HQ** in ethanol and mixed solvent
6. DLS characterization of the **TriPE(OH)-8HQ** in ethanol and mixed solvent
7. Selectivity of probes toward Zn^{2+}
8. Competitive experiment results of **TriPE(OH)-8HQ**
9. The process of protonation and deprotonation of **TPE(OH)-8HQ**
10. Mass spectra analysis for probes- Zn^{2+} complex
11. Calculation of the binding constant
12. Calculation of the limit of detection
13. Comparison of Zn^{2+} probes
14. References

1. Experimental section

Materials and instruments

Ethanol was purified prior to use. Other reagents and chemicals were purchased from commercial suppliers and used without further purification. ^1H NMR and ^{13}C NMR spectra were obtained on a Bruker AVANCE III 400 MHz Superconducting Fourier in DMSO- d_6 or CDCl_3 solution with TMS as an internal standard. Mass spectra (ES-MS) were obtained on Ultra High Performance Liquid Chromatography Tandem Triple Quadrupole Mass Spectrometer (*TSQ Endura). The IR (KBr pellet) spectrum was recorded (400–4000 cm^{-1} region) on a Nicolet Magna 750 FT-IR spectrometer. Emission Spectra were performed by steady-state fluorescence spectrometer (Edinburgh Instruments). UV-vis spectra were recorded on Lambda 20 UV-vis Spectrometer (PerkinElmer, Inc, USA). Stock solutions of various metal ions ($1 \times 10^{-3}\text{M}$) were prepared using chloride salts, except Ag^+ (AgNO_3). A stock solution of probes ($1 \times 10^{-3}\text{M}$) was prepared and then the stock solution was diluted 100 times.

2. Synthesis routes and Characterization



Scheme S1. The synthesis ways of these probes were according to previous reports.

Synthetic procedures:

- (a) $\text{Pd}(\text{PPh}_3)_4$, K_2CO_3 , toluene / MeOH, 75°C , reflux over night under N_2 atmosphere;
- (b) 1) 2-Methyl-8-hydroxyquinoline, Ac_2O , 140°C , reflux over night under air atmosphere;
2) pyridine, H_2O , 140°C , reflux over 3h under air atmosphere;
- (c) Zn powder, titanium tetrachloride, degassed THF, 80°C , reflux for 5.5 hours under N_2 atmosphere;
- (d) 1,3,5,7 -tetraazaadamantane, CH_3COOH , 90°C , reflux for 3 hours under air atmosphere;
- (e) CH_3I , K_2CO_3 , acetone, 65°C , reflux over night under N_2 atmosphere.

2.1 Synthesis of 4-(1,2,2-triphenylvinyl)benzaldehyde (I)^[1]:

2-bromo-1,1,2-tristyrene (3.36 g, 10 mmol), 4-formylphenylboronic acid (1.94 g, 13 mmol), K_2CO_3 (4.14 g, 30 mmol), $Pd(PPh_3)_4$ (0.064 g, 0.08 mmol) and 120 mL methanol-toluene (1:1, v/v) mixed solution was added to a 250 mL round bottom flask, stirred under N_2 at 75 °C for 16 hours. After completion of the reaction, it was cooled to room temperature and removal of solvent from the reaction mixture followed by purification through column chromatography using petroleum ether / ethyl acetate (8:1, v/v) as eluent after extraction, dried in vacuo to give a white solid, Yield: 3.24 g (89%). 1H NMR (400 MHz, $CDCl_3$) δ 9.90 (s, 1H), 7.61 (d, J = 8.0 Hz, 2H), 7.19 (d, J = 8.0 Hz, 2H), 7.16–7.07 (m, 9H), 7.07–6.96 (m, 6H). ^{13}C NMR (101 MHz, $CDCl_3$) δ 191.9, 150.5, 143.0, 142.9, 139.8, 134.3, 131.9, 131.3, 131.2, 129.1, 127.9, 127.9, 127.7, 127.0, 126.9, 126.9.

Synthesis of 4-(1,2,2-triphenylvinyl)phenol (IV): dried in vacuo to give a white solid, Yield: 71.7%. 1H NMR (400 MHz, DMSO) δ 9.39 (d, J = 10.4 Hz, 1H), 7.17 (m, 9H), 7.00 (m, 5H), 6.80 (m, 3H), 6.55 (d, J = 8.6 Hz, 2H). ^{13}C NMR (101 MHz, DMSO) δ 157.8, 156.4, 144.2, 144.1, 141.1, 139.6, 134.2, 132.4, 131.2, 131.2, 131.1, 129.8, 128.3, 128.2, 128.2, 126.9, 126.7, 119.3, 115.7, 115.1.

2.2 Synthesis of (E)-4-(1,2-diphenylvinyl)phenol (II) [2]:

benzaldehyde (1.06 g, 10 mmol), 4-hydroxybenzophenone (1.98 g, 10 mmol), Zn powder (6.5 g, 20 mmol) dissolved in degassed THF and then stir at room temperature for 1 hour under vacuum. After adding titanium tetrachloride (5.2 mL, 50 mmol) and then stirred at room temperature for 1 hour. Finally, stirred under N_2 at 80 °C for 5.5 hours. It was cooled to room temperature and removal of solvent from the reaction mixture followed by purification through column chromatography using petroleum ether / ethyl acetate (10:1, v/v) as eluent after extraction, dried in vacuo to give a white solid, Yield: 0.88 g (32.4%). 1H NMR (400 MHz, $CDCl_3$) δ 8.13 (m, 1H), 7.16 (m, 15H). ^{13}C NMR (101 MHz, DMSO) δ 156.4, 144.2, 144.1, 141.1, 139.6, 134.2, 132.4, 131.2, 131.2, 131.1, 128.3, 128.2, 128.1, 126.9, 126.7, 115.1.

2.3 Synthesis of 2-hydroxy-5-(1,2,2-triphenylvinyl)benzaldehyde (V) [3]:

TPE-OH (1.0 g, 3 mmol)(II) was added to 50 ml of acetic acid at room temperature and stirred slightly, hexamethylenetetramine (2.1 g, 15 mmol) was added to the reaction system after dissolving. The reaction was refluxed for 3 hours under air atmosphere. After the reaction was stopped, removal of solvent from the reaction mixture followed by purification through column chromatography using petroleum ether / ethyl acetate (5:1, v/v) as eluent after extraction, dried in vacuo to give a yellow solid. Yield: 0.55g (48.8%). 1H NMR (400 MHz, DMSO) δ 10.68 (s, 1H), 10.11 (s, 1H), 7.44 (t, J = 5.9 Hz, 1H), 7.23 (s, 1H), 7.11 (m, 9H), 6.98 (dd, J = 12.8, 8.0 Hz, 6H), 6.74 (m, 1H). ^{13}C NMR (101

MHz, DMSO) δ 191.3, 159.9, 143.6, 143.6, 143.3, 140.9, 139.8, 139.1, 134.9, 131.3, 131.2, 131.1, 131.1, 128.4, 128.4, 128.3, 127.2, 127.1, 126.9, 122.3, 117.2.

(E)-5-(1,2-diphenylvinyl)-2-hydroxybenzaldehyde (III): dried in vacuo to give a yellow solid, Yield: 40.7%. ^1H NMR (400 MHz, DMSO) δ 10.89 (s, 1H), 10.24 (d, $J = 2.3$ Hz, 1H), 7.54 (m, 1H), 7.35 (m, 5H), 7.08 (m, 8H).

2.4 Synthesis of 2-methoxy-5-(1,2,2-triphenylvinyl)benzaldehyde (VI) [4]:

The K_2CO_3 (0.27 g, 2 mmol) was added to a solution of compound (V) (0.37 g, 1 mmol) in acetone (20 mL) and the mixture was stirred for 0.5 h. Then the methyl iodide (0.28 g, 2 mmol) was added dropwise and stirred overnight at 65 °C. Removal of solvent from the reaction mixture followed by purification through column chromatography using petroleum ether / ethyl acetate (8:1, v/v) as eluent, dried in vacuo to give a light yellow solid. Yield: 0.56g (81.4%). ^1H NMR (400 MHz, DMSO) δ 10.20 (s, 1H), 7.28 (d, $J = 2.4$ Hz, 1H), 7.23 (dd, $J = 8.7, 2.4$ Hz, 1H), 7.13 (m, 9H), 6.99 (m, 7H), 3.84 (s, 3H). ^{13}C NMR (101 MHz, DMSO) δ 189.2, 160.6, 143.5, 143.4, 143.3, 141.3, 139.5, 139.0, 135.9, 131.2, 131.1, 131.1, 130.3, 128.5, 128.4, 128.3, 127.2, 127.2, 127.0, 123.9, 112.7, 56.4.

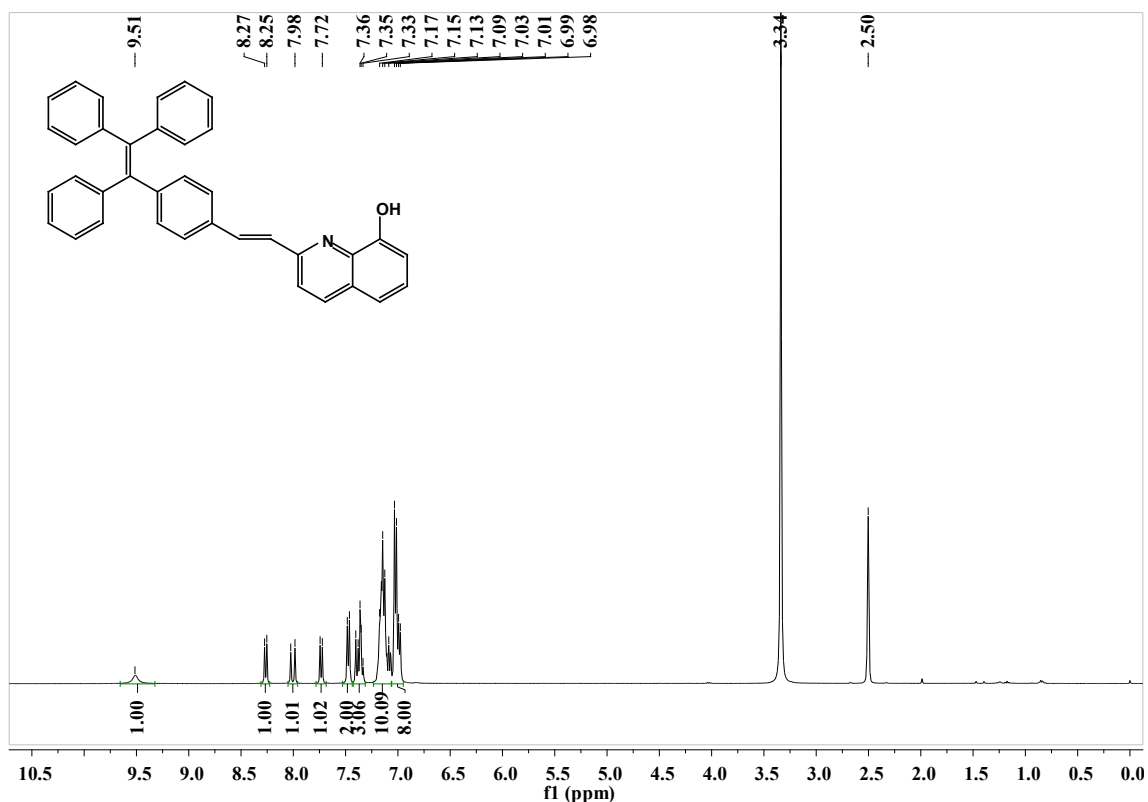


Fig. S1. ^1H NMR spectrum of TPE-8HQ

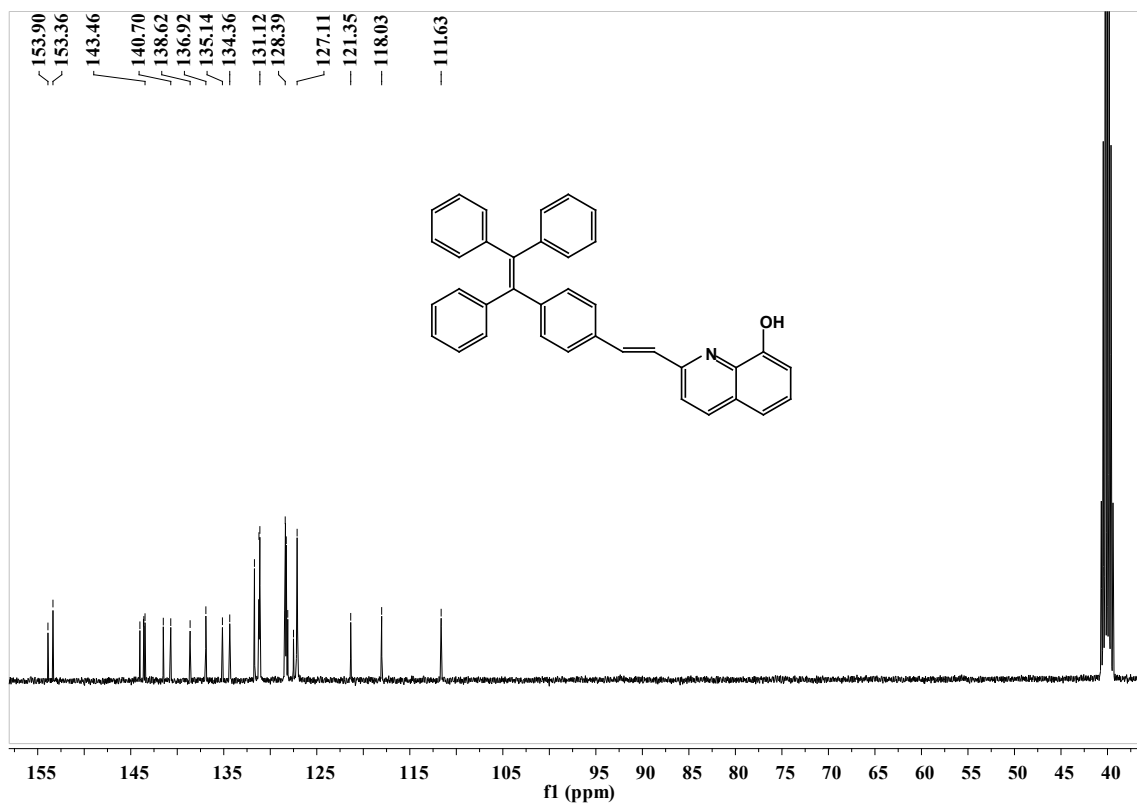


Fig. S2. ¹³C NMR spectrum of TPE-8HQ

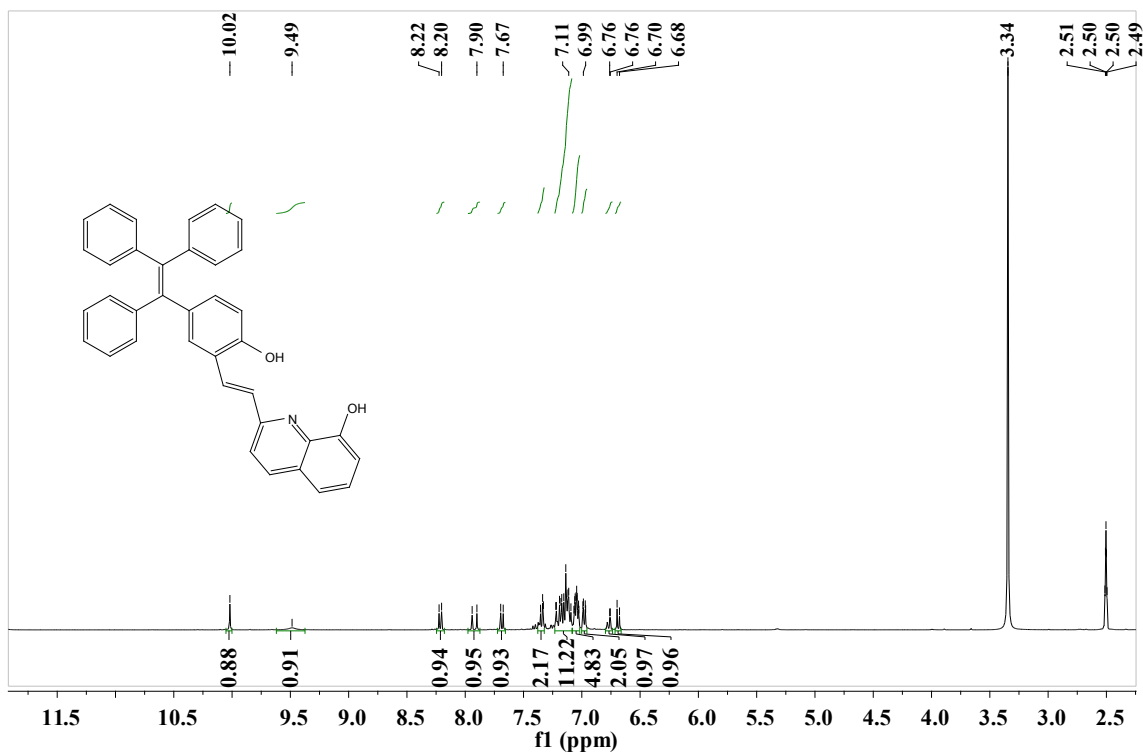


Fig. S3. ¹H NMR spectrum of TPE(OH)-8HQ.

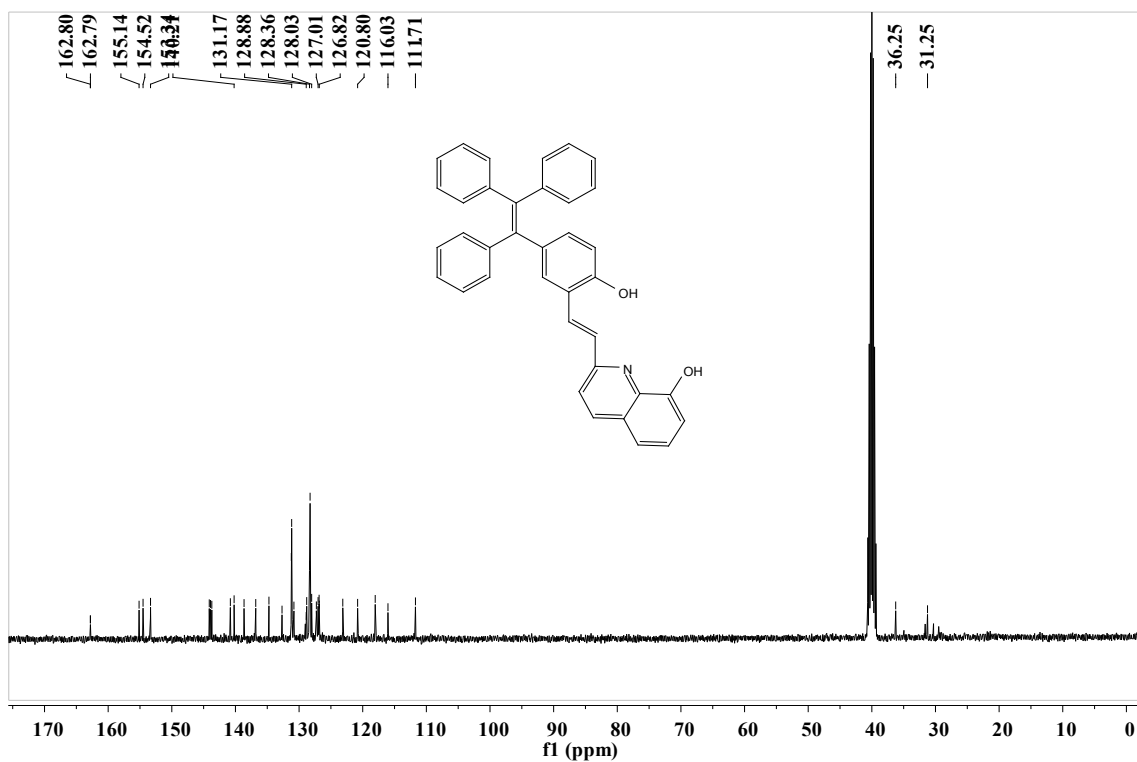


Fig. S4. ^{13}C NMR spectrum of TPE(OH)-8HQ.

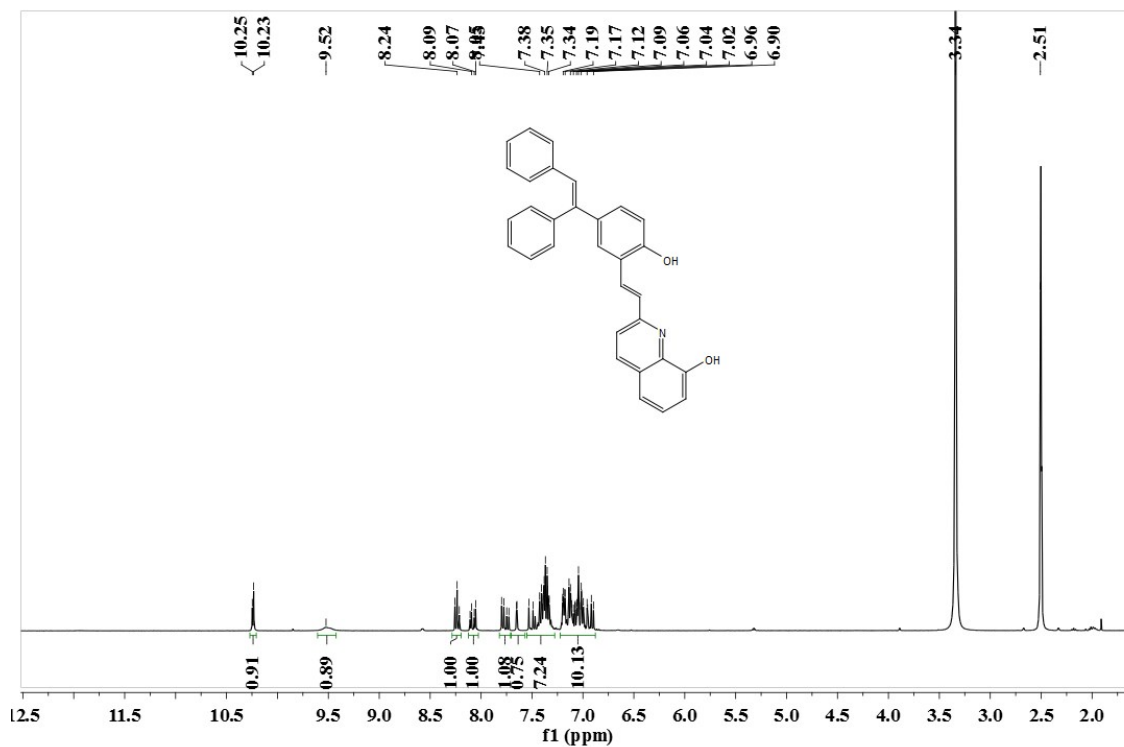


Fig. S5. ^1H NMR spectrum of TriPE(OH)-8HQ.

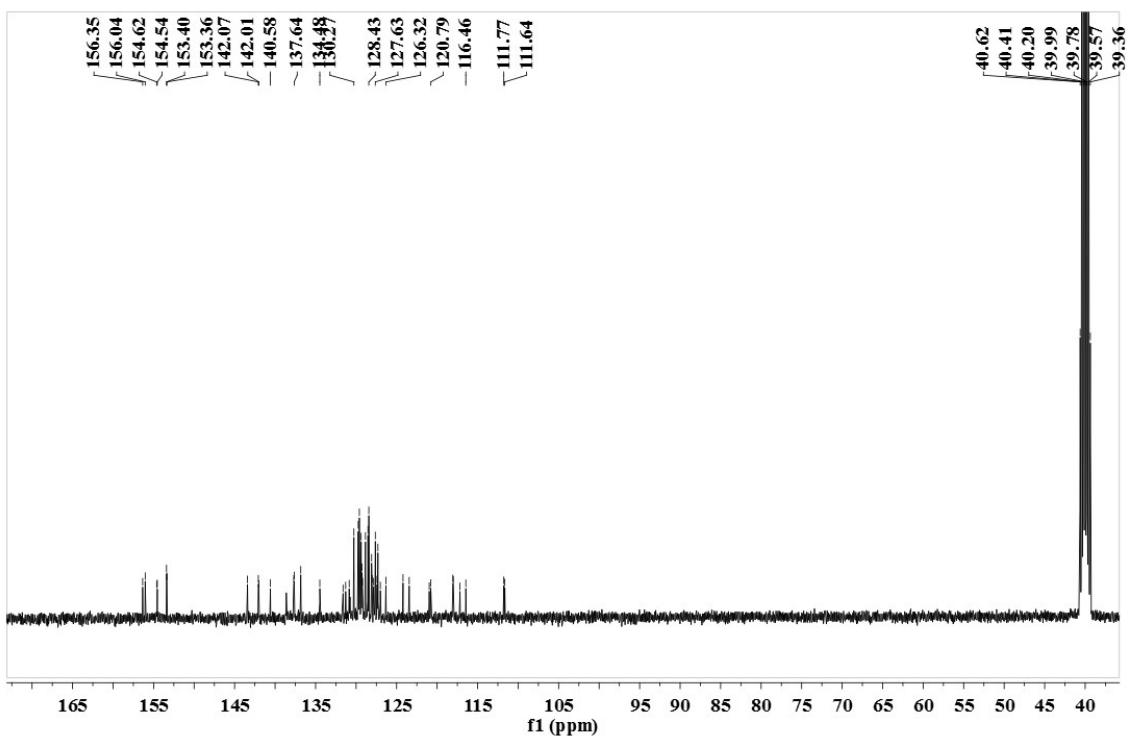


Fig. S6. ^{13}C NMR spectrum of TriPE(OH)-8HQ.

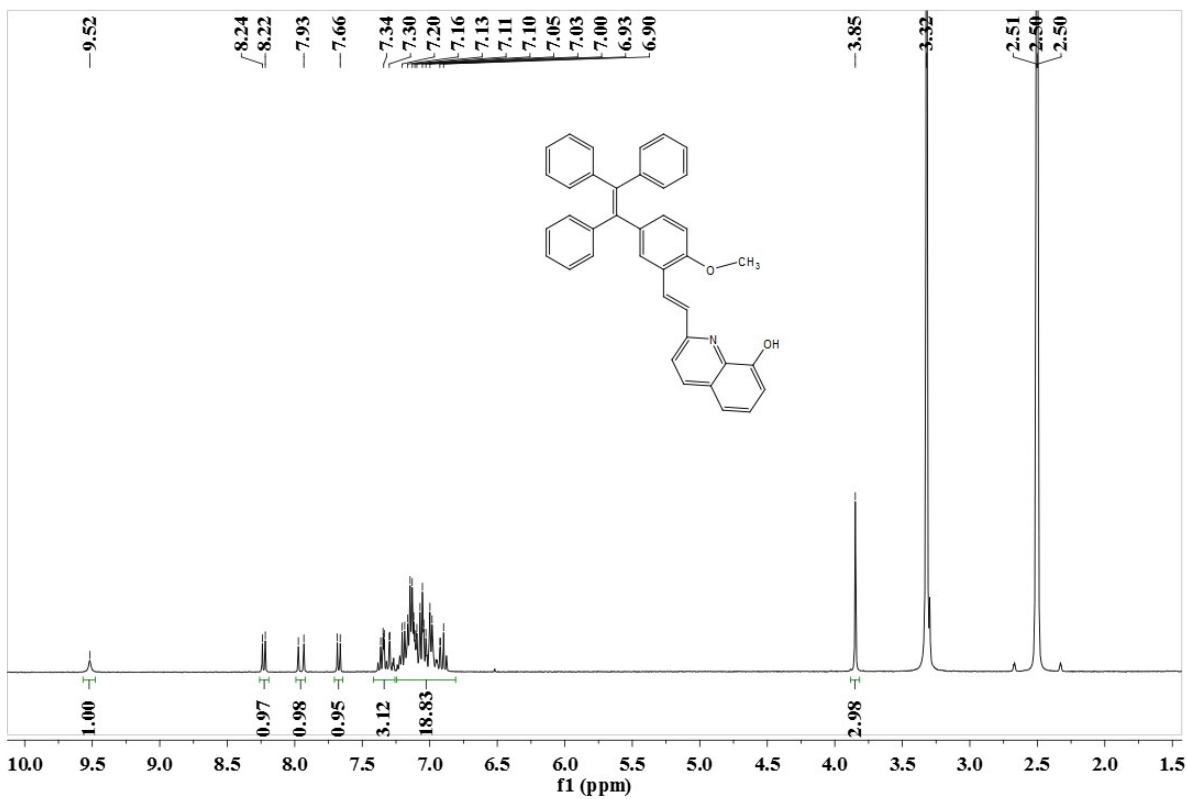


Fig. S7. ^1H NMR spectrum of TPE(OCH₃)-8HQ.

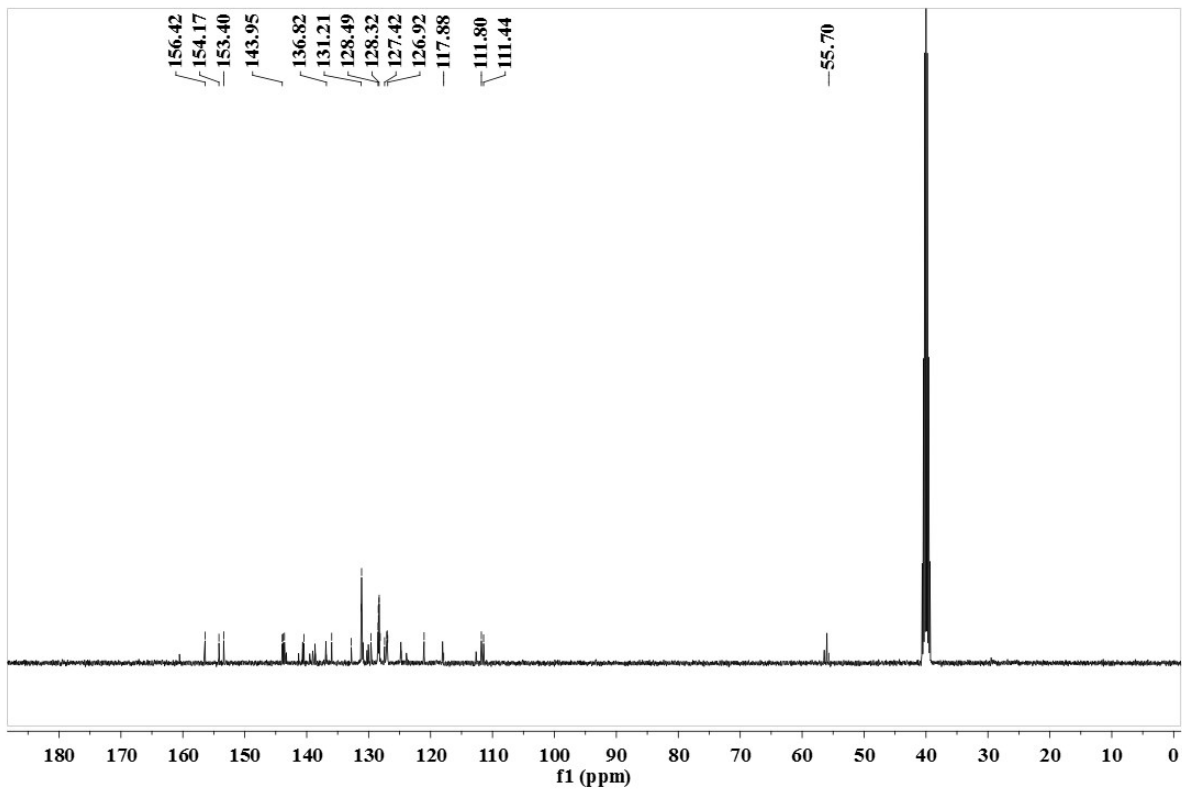


Fig. S8. ^{13}C NMR spectrum of TPE(OCH₃)-8HQ.

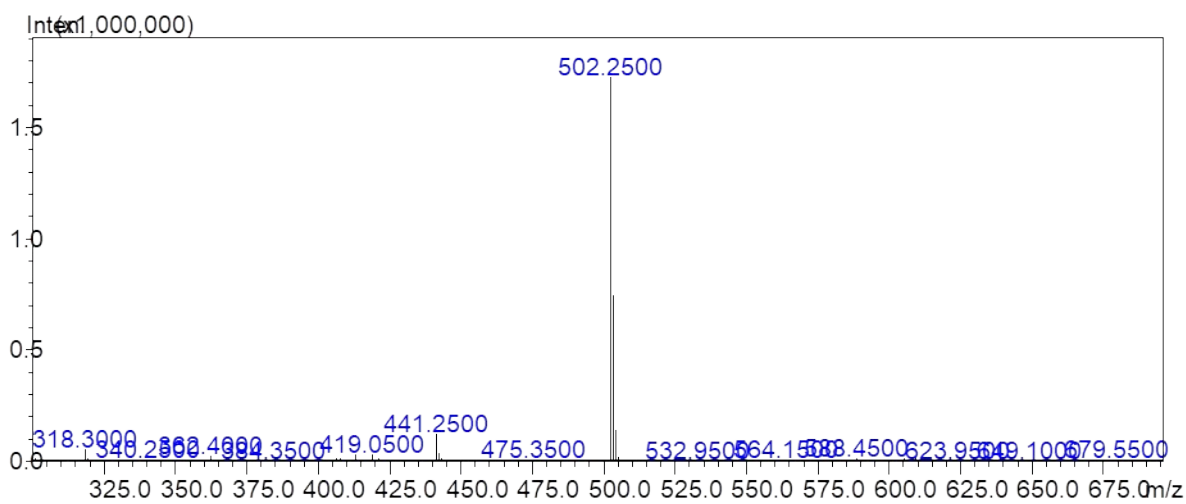


Fig. S9. Mass spectrum of TPE-8HQ

A #5 RT: 0.09 AV: 1 NL: 3.84E6
T: + c APCI Q1MS [200.000-1500.000]

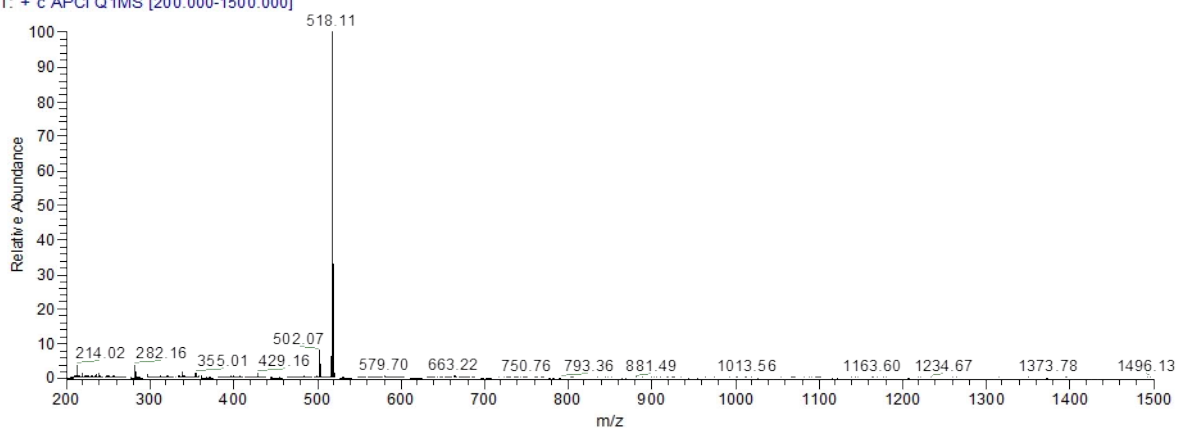


Fig. S10. Mass spectrum of TPE(OH)-8HQ

TriPE(OH)8HQ 2019120309451e #7 RT: 0.08 AV: 1 SB: 2 0.05, 0.13 NL: 2.63E6
F: + c ESI Q1MS [100.000-800.000]

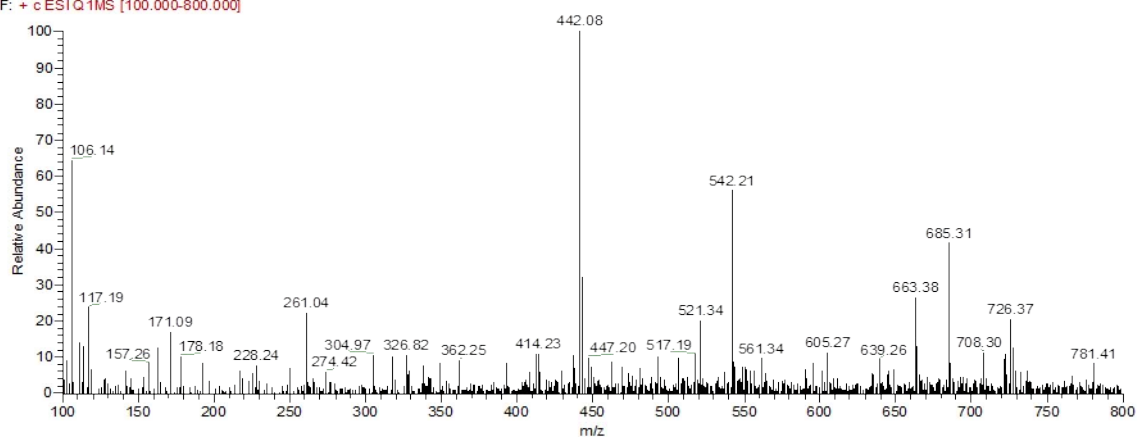


Fig. S11. Mass spectrum of TriPE(OH)-8HQ

TPE #7 RT: 0.09 AV: 1 NL: 1.24E7
F: + c ESI Q1MS [200.000-1000.000]

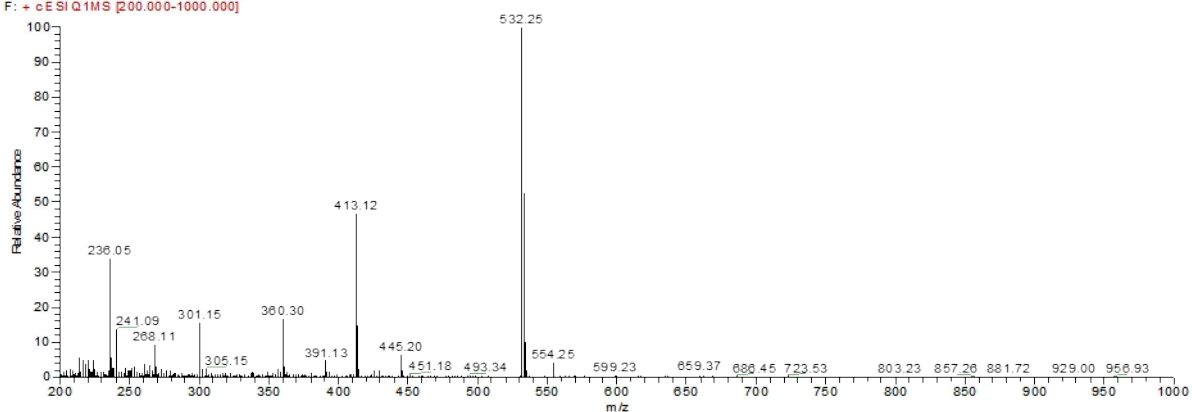


Fig. S12. Mass spectrum of TPE(OCH₃)-8HQ

3. IR spectrum of probe TPE(OH)-8HQ

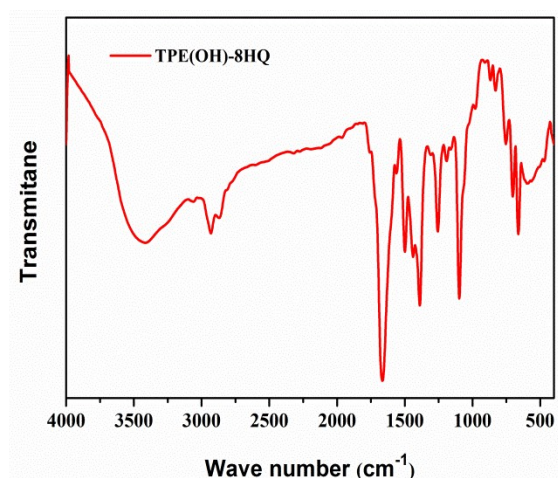


Fig. S13. IR spectrum of probe TPE(OH)-8HQ.

4. DLS characterization of the TPE-8HQ in ethanol and mixed solvent

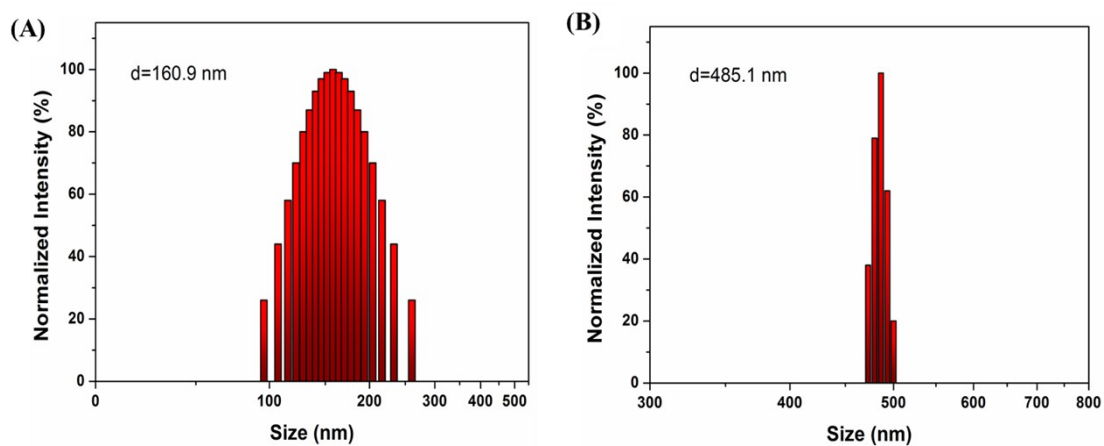


Fig.S14. DLS characterization of the TPE-8HQ in ethanol and mixed solvent (ethanol /H₂O = 9:1, v/v, 10 μ M).

5. DLS characterization of the TPE(OH)-8HQ in ethanol and mixed solvent

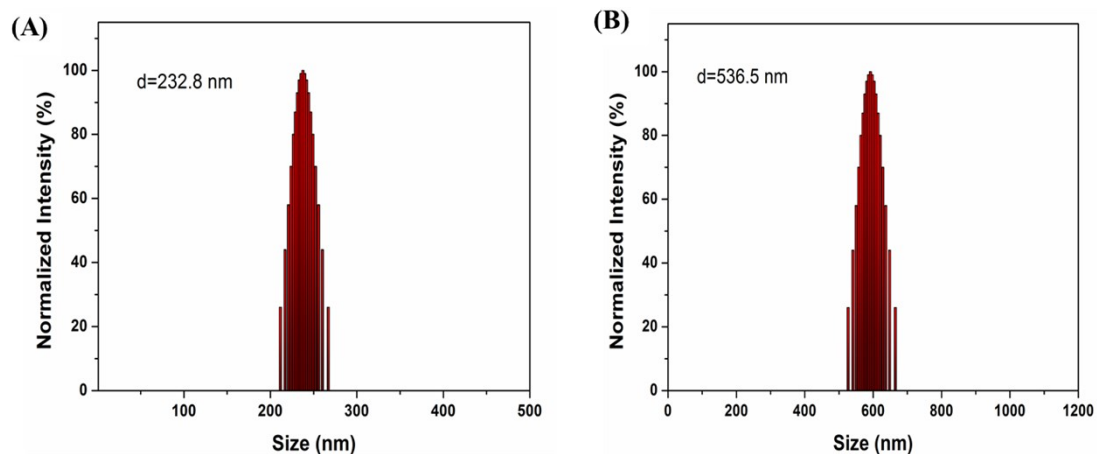


Fig.S15. DLS characterization of the TPE(OH)-8HQ in ethanol and mixed solvent (ethanol /H₂O = 9:1, v/v, 10 μM).

6. DLS characterization of the TriPE(OH)-8HQ in ethanol and mixed solvent

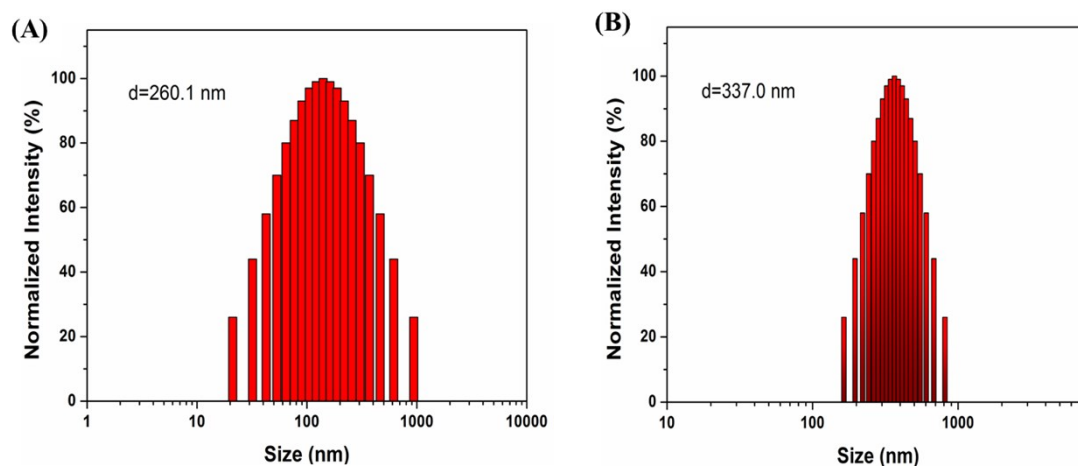
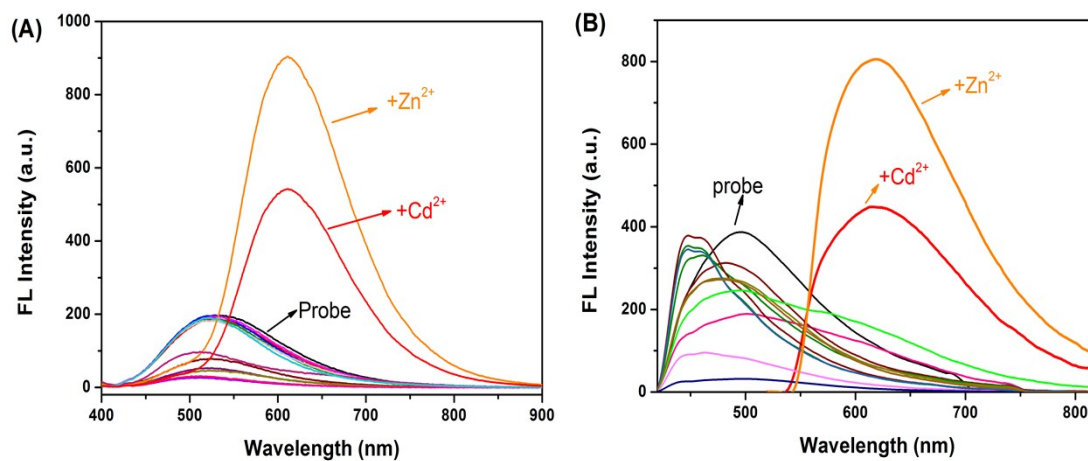


Fig.S16. DLS characterization of the TriPE(OH)-8HQ in ethanol and mixed solvent (ethanol /H₂O = 9:1, v/v, 10 μM).

7. Selectivity of probes toward Zn²⁺



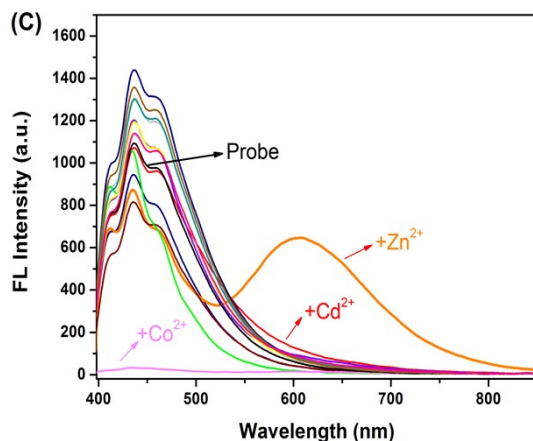


Fig.S17. Fluorescence emission spectra for (A) TPE-8HQ, (B) TPE(OCH₃)-8HQ and (C) TriPE(OH)-8HQ in C₂H₅OH /H₂O (9:1, v/v, 10 μM) after the addition of 10.0 eq of various metal ion ($\lambda_{\text{ex}} = 380 \text{ nm}$).

8. Competitive experiment results of TriPE(OH)-8HQ

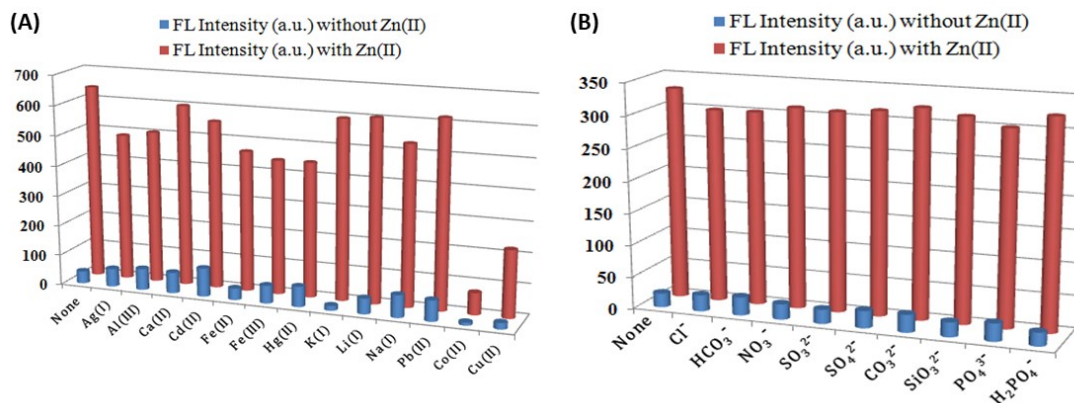


Fig. S18. (A) The fluorescent intensity at 605 nm of TriPE(OH)-8HQ (10 μM) with 50 μM of various metal ions, and then added 10 μM of Zn²⁺ in C₂H₅OH /H₂O (9:1, v/v) solution. (B)The fluorescent intensity of TriPE(OH)-8HQ (10 μM) with 50 μM of various anions, and then added 10 μM of Zn²⁺ in C₂H₅OH /H₂O (9:1, v/v) solution. ($\lambda_{\text{ex}}=380\text{nm}$).

9. The process of protonation and deprotonation of TPE(OH)-8HQ

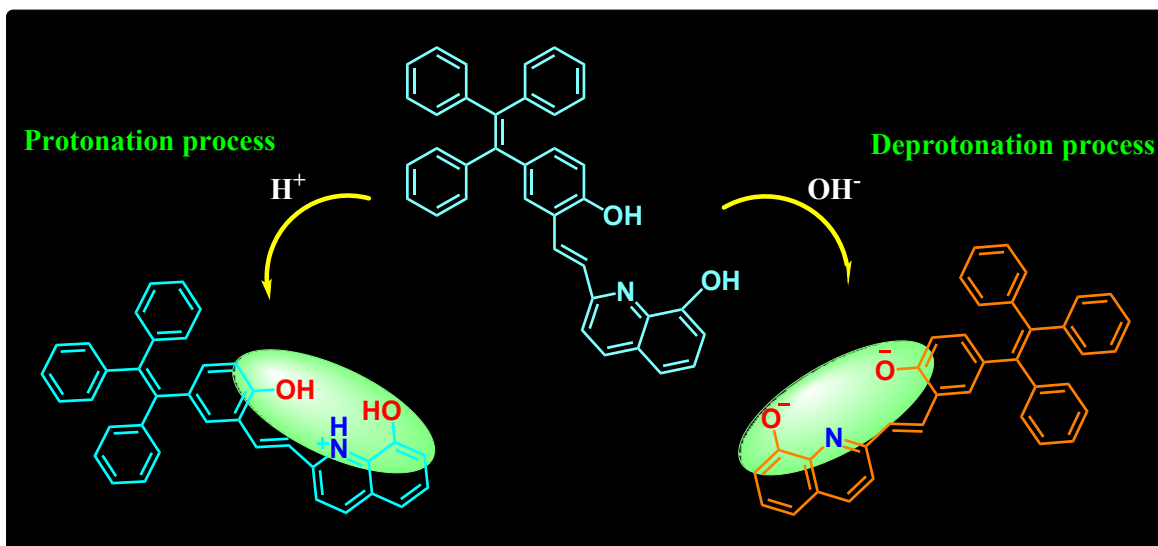
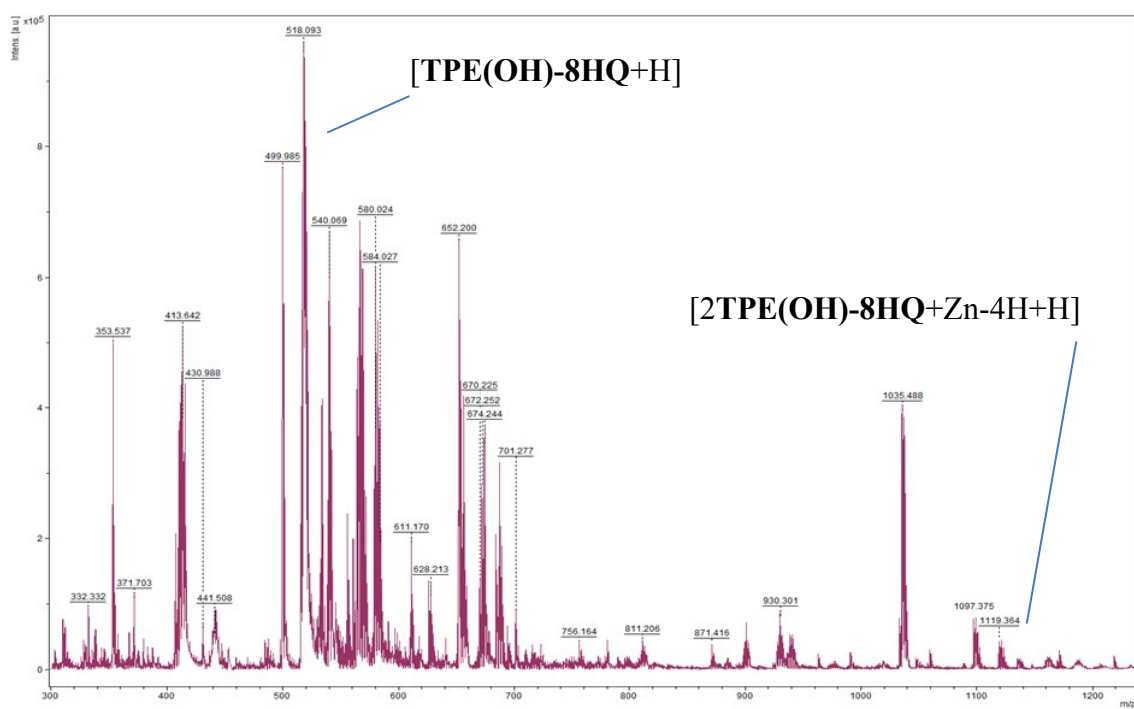


Fig. S19. The process of protonation and deprotonation of TPE(OH)-8HQ

10. Mass spectra analysis for probes-Zn²⁺ complex



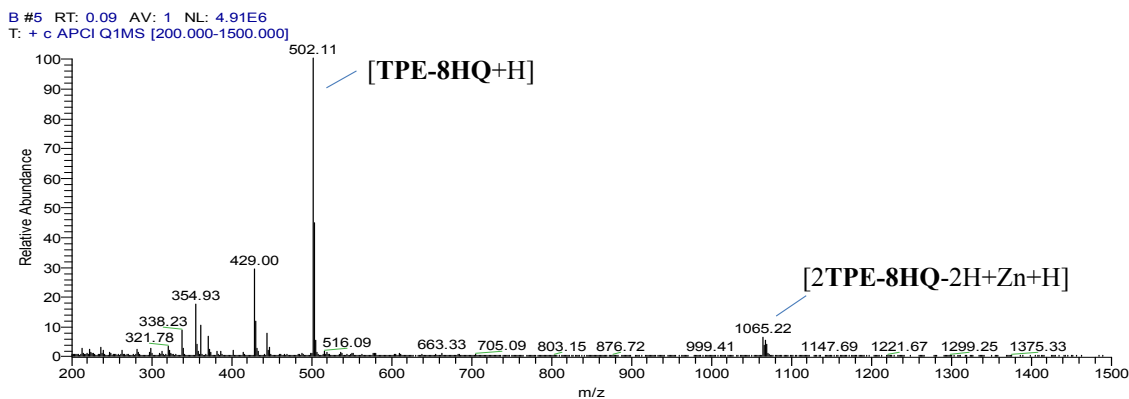


Fig. S20. Mass spectrum of TPE(OH)-8HQ(top) and TPE-8HQ(bottom) after added Zn^{2+} (5 equiv.) in the THF solution, indicating that the formation of a 2:1 probes- Zn^{2+} complex.

11. Calculation of the binding constant

Where K is the binding constant^[5], ΔI is the difference between the intermediate coordination emission intensity and the probe emission intensity without the Zn^{2+} ion; ΔI_{max} is the fully coordinated emission intensity and the probe emission intensity without the Zn^{2+} ion; K is the binding constant; $[M]$ is the Zn^{2+} ion concentration. The calculated binding constant K between TPE(OH)-8HQ and Zn^{2+} ion was $2.17 \times 10^5 M^{-1}$, and the binding constant indicates that the probe has strong binding ability to Zn^{2+} ions.

$$\frac{1}{\Delta I} = \frac{1}{\Delta I_{max}} + (1/K[M])(1/\Delta I_{max}) \quad \text{Eq. S1}$$

12. Calculation of the limit of detection

LOD is the limit of detection which was calculated based on equation (Eq.S2)^[6], where σ is the standard deviation of the blank probe solution, S is the slope of the calibration plot in Fig.7(B).

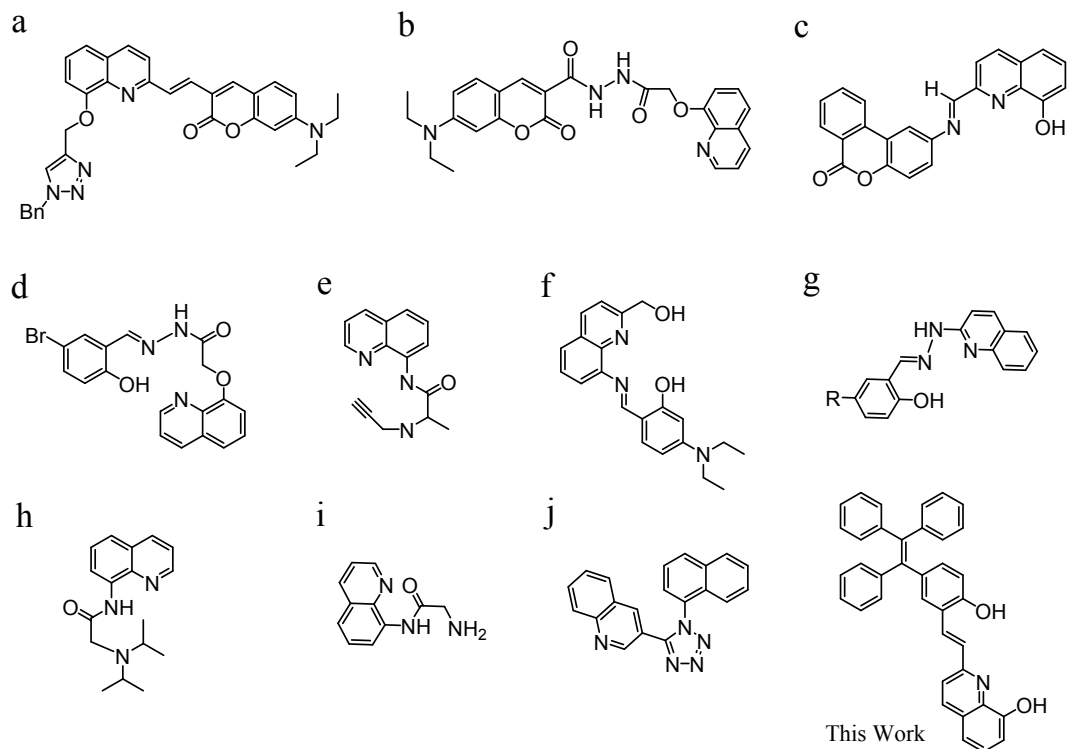
$$LOD = \frac{3\sigma}{s} \quad \text{Eq. S2}$$

13. Comparison of Zn^{2+} probes

Table S1

The structures of some quinoline contained fluorescent probes for Zn²⁺ in the previous literatures.

Comparison of some quinoline contained fluorescent probes for Zn²⁺ in the literatures.



Probe	λ_{em}/nm	LOD/ $10^{-6}M$	Stokes Shift /nm	Reference
a	516	0.98	25	Ref. [7]
b	469	0.6	59	Ref. [8]
c	425	10	75	Ref. [9]
d	*	0.02	80	Ref. [10]
e	416	0.063	82	Ref. [11]
f	458	0.027	96	Ref. [12]
g	502	0.22	105	Ref. [13]
h	*	0.041	151	Ref. [14]
i	420	1.6	160	Ref. [15]
j	460	0.02	170	Ref. [16]
This Work	470	0.164	289	

“*” — The data is not given in the literature.

1. J. Li, N. Kwon, Y. Jeong, S. Lee, G. Kim, J. Yoon. Aggregation-Induced Fluorescence Probe for Monitoring Membrane Potential Changes in Mitochondria. *ACS applied materials & interfaces*, 2018, **10**(15): 12150-12154.
2. B. Ganchev, G. Heinkele, R. Kerb, M. Schwab, T. Mudter. Quantification of clomiphene metabolite isomers in human plasma by rapid-resolution liquid chromatography–electrospray ionization–tandem mass spectrometry. *Analytical and bioanalytical chemistry*, 2011, **400**(10): 3429-3441.
3. H.W. Liu, K. Li, X.X. Hu, L.M. Zhu, Q.M. Rong, Y.C. Liu, X.B. Zhang, J. Hasserodt, F.L. Qu, W.H. Tan. In Situ Localization of Enzyme Activity in Live Cells by a Molecular Probe Releasing a Precipitating Fluorochrome. *Angewandte Chemie-International Edition*, 2017, **56**, 11788-11792.
4. K. Li, Y. Li, D. Zhou, Y. Fan, H. Guo, T.Y. Ma, J.C. Wen, D. Liu, L.X. Zhao. Synthesis and biological evaluation of quinoline derivatives as potential anti-prostate cancer agents and Pim-1 kinase inhibitors. *Bioorganic & medicinal chemistry*, 2016, **24**, 1889-1897.
5. A.K. Mandal, M. Suresh, P. Das, E. Suresh, M. Baidya, S.K. Ghosh, A. Das. Recognition of Hg²⁺ Ion through Restricted Imine Isomerization: Crystallographic Evidence and Imaging in Live Cells. *Organic Letters*. 2012, **14**, 2980-2983.
6. J. Zhang, Y. Zhou, W. Hu, L. Zhang, Q. Huang, T.S. Ma. Highly selective fluorescence enhancement chemosensor for Hg²⁺ based on rhodamine and its application in living cells and aqueous media. *Sensors and Actuators B: Chemical*, 2013, **183**, 290-296.
7. G.F. Wu, Q. Gao, M.G. Li, X. Tang, K.W.C. Lai, Q.X. Tong. A ratiometric probe based on coumarin-quinoline for highly selective and sensitive detection of Zn²⁺ ions in living cells. *Journal of Photochemistry and Photobiology A: Chemistry*, 2018, **355**, 487-495.
8. T.T. Kang, H.P. Wang, X.J. Wang, L.H. Feng. A facile Zn(II) probe based on intramolecular charge transfer with fluorescence red-shift. *Microchemical Journal*, 2019, **148**, 442-448.
9. N Roy, A Dutta, P Mondal, P.C. Paul, T.S. Singh. A new coumarin based dual functional chemosensor for colorimetric detection of Fe³⁺ and fluorescence turn-on response of Zn²⁺. *Sensors and Actuators B: Chemical*, 2016, **236**, 719-731.
10. K. Ponnuvel, M. Kumar, V. Padmini. RETRACTED: A new quinoline-based chemosensor for Zn²⁺ ions and their application in living cell imaging. *Sensors and Actuators B: Chemical*, 2016, **227**, 242-247.
11. H.H. Song, Z. Zhang. A quinoline-based ratiometric fluorescent probe for discriminative detection of Zn²⁺ and Cd²⁺ with different binding modes, and its Zn²⁺ complex for relay sensing of pyrophosphate and adenosine triphosphate. *Dyes and Pigments*, 2019, **165**, 172-181.

12. J.X. Fu, Y.X. Chang, B. Li, H.H. Mei, K.X. Xu. An aminoquinoline based fluorescent probe for sequential detection of Zinc (II) and inorganic phosphate and application in living cell imaging. *Applied Organometallic Chemistry*, 2019, **15**, 1-9.
13. D. Maity, A. Mukherjee, S.K. Mandal, P. Roy. Modulation of fluorescence sensing properties of quinoline-based chemosensor for Zn²⁺: Application in cell imaging studies. *Journal of Luminescence*, 2019, **210**, 508-518.
14. H.Y. Liu, Y. Tan, Q.Z. Dai, H.D. Liang, J. Song, J. Qu, W.Y. Wong. A simple amide fluorescent sensor based on quinoline for selective and sensitive recognition of zinc(II) ions and bioimaging in living cells. *Dyes and Pigments*, 2018, **158**, 312-318.
15. K. Boonkitpatarakul, A. Smata, K. Kongnukool, S. Srisuichan, K. Chainok, M. Sukwattanasinit. An 8-aminoquinoline derivative as a molecular platform for fluorescent sensors for Zn(II) and Cd(II) ions. *Journal of Luminescence*, 2018, **198**, 59-67.
16. K. Ponnuvel, V. Padmini, R. Sribalan. A new tetrazole based turn-on fluorescence chemosensor for Zn²⁺ ions and its application in bioimaging. *Sensors and Actuators B: Chemical*, 2016, **222**, 605-611.